JOURNAL OF CHEMICAL INFORMATION AND MODELING

Article

pubs.acs.org/jcim

Molecular Dynamics Simulations of the Interaction of Beta Cyclodextrin with a Lipid Bilayer

Wasinee Khuntawee,[†] Peter Wolschann,[‡,§] Thanyada Rungrotmongkol,[*,∥,⊥] Jirasak Wong-ekkabut,[*,#] and Supot Hannongbua[▽]

[†]Nanoscience and Technology Program, Graduate School, [∥]Ph.D. Program in Bioinformatics and Computational Biology, Faculty of Science, [⊥]Department of Biochemistry, Faculty of Science, and [▽]Computational Chemistry Unit Cell, Department of Chemistry, Faculty of Science, Chulalongkorn University, 254 Phayathai Road, Patumwan, Bangkok 10330, Thailand

[‡]Department of Pharmaceutical Technology and Biopharmaceutics, University of Vienna, 14 Althan Straße 14, Vienna 1090, Austria

[§]Institute of Theoretical Chemistry, University of Vienna, Währinger Straße 17, Vienna 1090, Austria

[#]Department of Physics, Faculty of Science, Kasetsart University, 50 Phahon Yothin Road, Chatuchak, Bangkok 10900, Thailand

Supporting Information

ABSTRACT: Beta cyclodextrin (βCD) is well-known as a potent drug carrier improving drug solubility, stability, and bioavailability. The water layer adjacent to the membrane surface and lipophilic domain itself are a controlling barrier for drug transport. However, the molecular details of the interaction between βCD and the lipid membrane has not yet been clearly explained. Here, molecular dynamics simulations were performed to visualize the interaction process of the βCD molecule with the lipid bilayer for six microseconds in total. Our results show that βCD passively diffuses into the lipid bilayer by pointing its open secondary rim toward the lipid polar groups and then remains at the phosphate and glycerol-ester groups with hydrogen bond formation. The information obtained from this study may suggest that the association of βCD at the cellular membrane plays an important role for the transfer of drug and the extraction of cholesterol.

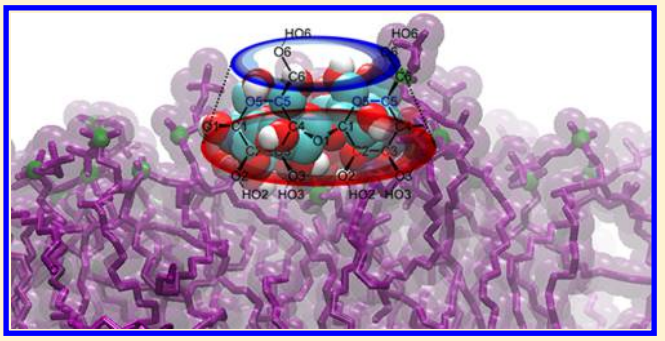

INTRODUCTION

Drug delivery systems (DDS) have been continuously developed with the aims to enhance therapeutic drug efficiency and consequently to reduce toxicity by the direct transportation to specific targets. Cyclodextrins (CDs) are used as potential drug carriers.[1] Natural CDs are αCD, βCD, and γCD, composed of six, seven, and eight units of D-glucopyranose, respectively, with α-1,4 linkages (Figure 1). βCD is widely used in pharmaceutical and food industries because of low cost, easy synthetic accessibility, and suitable cavity size (0.60−0.65 nm) for the inclusion of small- and medium-sized drugs.[2] βCD and some derivatives have been used in inclusion complexation with drugs, and they have been approved and marketed especially for oral drug delivery.[3] The structure of the βCD molecule is that of a truncated cone with a hydrophilic outer surface and a relatively hydrophobic nanocavity. Therefore, a poorly water-soluble molecule can be inserted into the CD's cavity leading to an increased solubility and consequently to a higher biological activity.

Based on biopharmaceutical drug classification, there are two main factors for efficient drug transport ability, the solubility and the permeation of the drug through biological membranes.[4] Many experimental and theoretical studies have demonstrated that the aqueous solubility enhancement of lipophilic drugs by

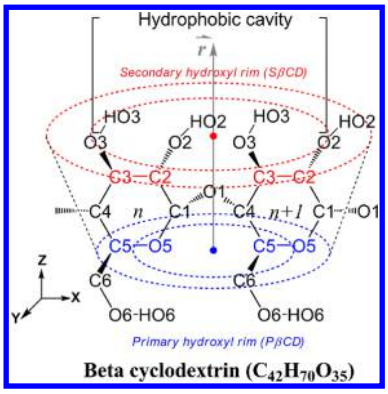

Figure 1. 2D structure of βCD showing the arrangement of glucose monomers. The atoms on the glucose ring representing the primary rim and the secondary rim are labeled in blue and red, respectively.

CDs inclusion leads to the increased drug efficacy.[5−10] The βCD supported drug delivery may occur via two mechanisms. First, the drug dissociates from the βCD and then adsorbs into the membrane surface. Second, the drug−βCD complex

Received: March 19, 2015
Published: August 24, 2015

DOI: 10.1021/acs.jcim.5b00152
J. Chem. Inf. Model. 2015, 55, 1894−1902

directly transfers into the membrane in which the association and permeability of βCD complexes are possibly controlled by the barrier of the unstirred water layer (UWL) at the membrane surface.[11,12] The drug−βCD complexes permeate through the UWL to reach the membrane surface via passive diffusion but may not get into the membrane interior due to their size and other physicochemical properties.[11−13] Actually, the binding of βCDs at the water−lipid interface has been experimentally proven by the extraction of cholesterol by βCDs.[14,15] To date, there is no detailed study as to how the unstirred water layer and the membrane itself influence the association of the drug−βCD complex. As a very important prestep for the understanding of drug delivery at the membrane, the interactions of βCDs with the membrane have to be investigated.

Molecular understanding of the complex biological systems have been achieved by molecular dynamics (MD) simulations, which provided reliable and reasonable results comparable to experiments.[16−19] The simulations in the lipid phase well described the interaction of small molecules with the lipid membrane.[16,20−24] Wei et al. showed the agreement of computational and experimental studies for the translocation of ribose and its two diastereomers into 1-palmitoyl-2-oleoyl-*sn*-glycero-3-phosphocholine (POPC).[25] Moreover, the MD simulations have been extended to investigate physicochemical properties, host−guest interaction, and self-aggregation of sugar oligomer as cyclodextrins in both gas and solution phases.[26−34] An understanding of CDs-based DDS as a drug loading can be carried out by the estimation of the binding affinity of drug to CD and complexity itself. The structure stability and phase solubility studies suggested that the hydrophobic molecule is bound properly in the cavity of CDs by 1:1,[35−38] 2:1,[37,39] and 2:2[40,41] stoichiometry. The study of the complex architecture of βCD with hydrochlorothiazide (HCT) concluded that the formation of the HCT−βCD complex was enthalpy driven and the inclusion mode of HCT was highly dependent on its ionization state.[42] On the other hand, the drug releasing may be described with the interactions of drug, CD, and the drug−CD complex with the lipid membrane.[11] The studies of the exposing cells or model membranes to CDs have shown that the membrane cholesterol was removed from the lipid rafts.[11,14,15,43−49] The MD simulation also showed that βCD can rapidly adsorb on the membrane with a consequence of cholesterol extraction. The ability of cholesterol extraction by head-to-head dimer βCD depended on the orientation, the distribution of βCD on the membrane surface, and the concentrations of cholesterol in the membrane.[48,49] The mechanism to remove cholesterol from the lipid membrane was described by Lopez et al.[48,49] The proper conformation for cholesterol extraction is that the hydroxyl rim of the βCD dimer bound to the membrane surface with hydrogen bonds. Moreover, the extraction energy was significantly reduced at low concentration of cholesterol because the lipids prevented the βCD-cholesterol interactions.[49] Although the extraction of cholesterol by CDs has been studied to some extent,[48,49] drug delivery and CD-lipid interaction are still not completely resolved. Therefore, a deeper understanding on βCD permeability in the biological membrane at the molecular level is required for the further development of CD-based drug delivery and drug release control. Here, we performed all-atom MD simulations with various starting geometries of βCD with regards to the POPC lipid bilayer model. The permeation behavior of βCD and its structure properties were of concern.

METHODOLOGY

System Preparation. MD simulations were performed with five different initial configurations as shown in Figure 2(a)-(e). In the BCD1-BCD3 systems, the βCD molecule with different orientations was located in the water phase at a distance of 3.5 nm in the *z* direction from the center of the bilayer. On the other hand, BCD4 and BCD5 represent the starting geometries when the βCD molecule is placed at the center of the lipid bilayer with parallel and perpendicular orientations, respectively. These setups allow us to study the behavior of βCD in the bilayer, and this technique has been widely used in the simulations of molecular transportation into the membrane.[50−52] In the case of BCD5, the hydroxyl rims of βCD closely interacted with lipid head groups. Note that this initial configuration may have an influence on the trajectory. A symmetric structure of the βCD molecule was taken from our previous study,[53] while the initial coordinates of the equilibrated 128 POPC bilayer were received from Tieleman's group (http://wcm.ucalgary.ca/tieleman/downloads/popc128b.pdb). All simulations were performed by using the GROMACS package version 4.5.5.[54] The POPC membrane was simulated by the modified Berger et al. parameters,[19,55] and the βCD molecule was described by GROMOS 53A6[56] (the carbohydrate force field is equivalent to GROMOS 45A4[57]). Note that a validation of the force field for βCD was carried out. The structural properties of βCD in water were compared with the result from the X-ray crystallography and also other MD simulations.[58−61] The general perspectives of βCD structural properties are in agreement with the previous studies as shown in Supporting Information Table S1. The POPC lipid bilayers were fully solvated by 7122 molecules of single point charge (SPC) water[62] in the simulation box size of 6.42 × 6.45 × 9.19 nm^3.

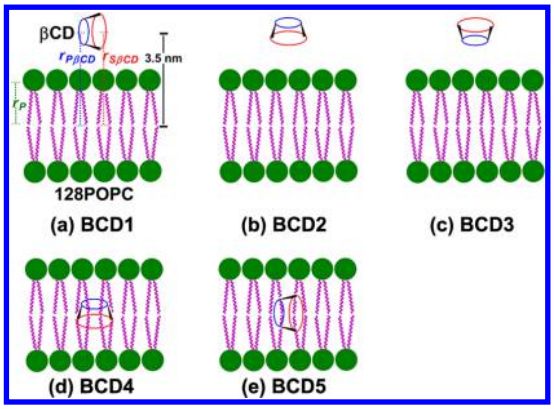

Figure 2. (a)-(c): Starting geometries of various orientations βCD at the membrane surface. (d)-(e): Starting geometries of various orientations βCD inside the membrane.

Molecular Dynamics Simulation. After the energy minimization with the steepest descent algorithm for 10000 steps, classical MD simulations were carried out with NPT ensemble (the particle number, pressure, and temperature were kept constant) over one microsecond, except for the BCD5 system, where the simulation was extended to two microseconds. At least equilibrated trajectories over 500 ns were used for analysis. The integration time step was set at 2 fs, and the trajectories were sampled every 2 ps. The periodic boundary was applied in all directions. βCD, lipid, and water molecules were separately thermostated at 298 K by the Parrinello-Bussi

DOI: 10.1021/acs.jcim.5b00152
J. Chem. Inf. Model. 2015, 55, 1894−1902

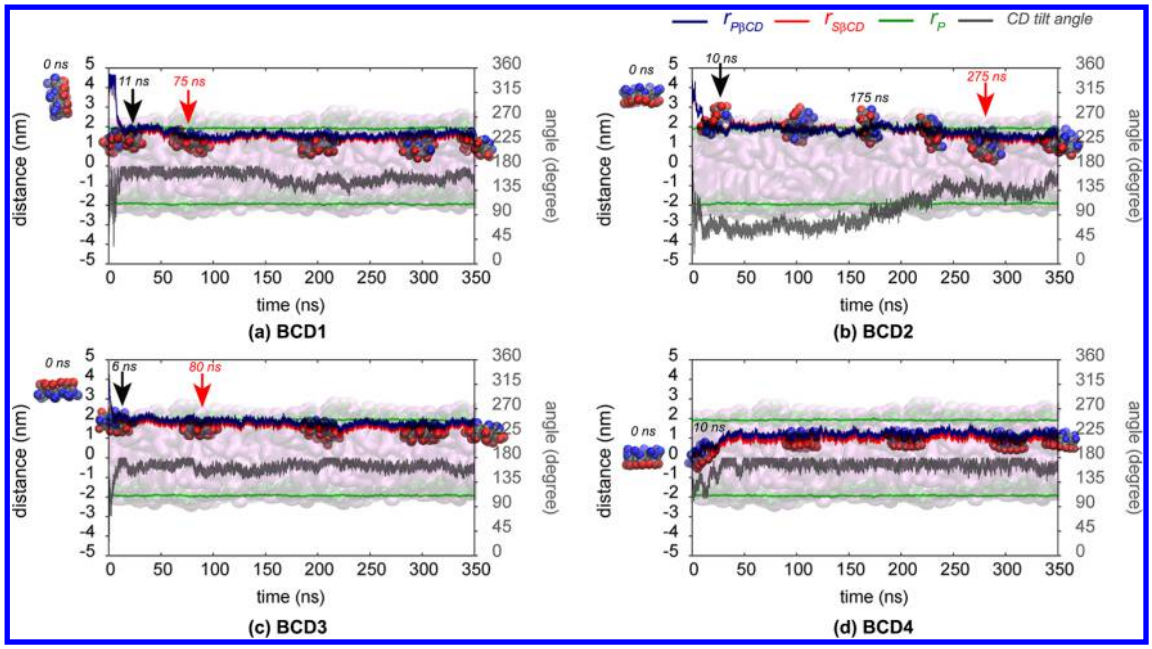

Figure 3. Closed-up for the first 350 ns of the permeation of βCD into the lipid bilayer for four simulations ((a) BCD1-(d) BCD4) using different initial structures. The distances as a function of time between the centers of the bilayer and both rims of the βCD molecule i.e. primary rim; $r_{P\beta CD}$ (blue) and secondary rim; $r_{S\beta CD}$ (red) are depicted. The βCD tilt angle and the distances of phosphate groups from the center of the bilayer for both leaflets (r_p) are plotted in gray and green, respectively. The snapshots of βCD at different simulation times are enclosed in the plots where the blue and red balls represent the atoms of the primary and secondary rims, respectively. The lipids of the bilayer are shown by purple rods, while their phosphorus atoms are depicted in green balls. The black and red arrows indicate the approaching and permeating time of βCD to the bilayer, respectively. The complete distances of the simulations are collected in Figure S1 in the Supporting Information.

velocity rescale algorithm.[63,64] Semi-isotropic pressure was applied by the Berendsen algorithm,[65] at an equilibrium pressure of 1 bar both in the *xy*-plane and in the *z*-direction (bilayer normal) with a time constant of 3.0 ps and a compressibility of 4.5×10^{-5} bar^{-1}. The Lennard-Jones and the real-space parts of electrostatic interactions were cut off at 1.0 nm. The particle mesh Ewald (PME) method[66−68] was used to compute long-range interactions with the reciprocal-space interactions evaluated on a 0.12 nm grid with cubic interpolation of order four. All bond lengths were constrained by the LINCS algorithm.[69] The used simulation protocol has been tested and validated to work well for lipid systems.[70,71] Molecular visualizations were done using Visual Molecular Dynamics (VMD) software.[72]

RESULTS AND DISCUSSION

The results of this study have been divided into three sections as follows: *I) The permeation and insertion of the βCD molecule into the lipid bilayer*; the βCD molecule permeation into the POPC lipid bilayer and the effect of the βCD molecule insertion on the bilayer were shown. *II) The interaction of the βCD molecule with the lipid bilayer*; the number of hydrogen bonds between the βCD molecule and the lipid bilayer were calculated to determine the binding interaction between βCD and lipids. In addition, the influence of βCD on lipid bilayer properties was analyzed in terms of a 2D-density map of βCD and POPC as well as local lipid thickness. In the last section, *III) The conformational change of the βCD molecule*; the conformation and structural stability of the βCD molecule at water, water−lipid interface, and lipid bilayer were considered.

I. The Permeation and Insertion of the βCD Molecule into the Lipid Bilayer. The βCD molecule was initially set far away from the bilayer center (around 3.5 nm) to avoid the bias of the interactions between the βCD molecule and the lipid bilayer (as seen in Figure 2). This allowed the βCD to move and rotate freely in aqueous solution before approaching the bilayer surface. To study the permeation of the βCD molecule into the lipid bilayer, the distances in the *z*-axis of the βCD molecule ($r_{\beta CD}$) and its rims ($r_{P\beta CD}$ and $r_{S\beta CD}$ for primary and secondary hydroxyl sides, respectively) away from the lipid bilayer's center were determined as a function of time (as seen in Figure 3). The center of mass (COM) of all lipid molecules, the COM of all atoms in the βCD molecule, the COM of C5 and O5 atoms, and the COM of C2 and C3 atoms were defined as the bilayer center, the βCD center, the primary rim center, and the secondary rim center, respectively. The tilt angle of the βCD molecule is characterized by the angle between vector $\vec{r}$ (the vector pointing from the COMs of the primary to the secondary rims, as seen in Figure 1) and the bilayer normal. The definitions of all mentioned parameters are illustrated in Figure 1 and Figure 2(a).

Figure 3 shows that the βCD molecule in the aqueous phase spontaneously moved toward the POPC bilayer and approached the bilayer surface within the first 15 ns. For the BCD1 and BCD3 systems, the βCD molecule attached to the bilayer with the secondary rim and readily permeated into the lipid bilayer within approximately 100 ns. The βCD remained underneath the phosphate group for the rest of the simulation time (Figure S1). For the BCD2 system, the βCD molecule first approached the bilayer surface with the primary rim, but it did not permeate into the bilayer over a hundred nanoseconds. After 175 ns simulation time, the βCD molecule rotated to have the secondary rim associated with the bilayer surface with the consequence of the βCD permeation within a few tens of nanoseconds as illustrated in Figure 3(b). After 500 ns, all βCD molecules are located in the region between phosphate and

DOI: 10.1021/acs.jcim.5b00152
J. Chem. Inf. Model. 2015, 55, 1894−1902

glycerol-ester groups with the orientation of the secondary rim pointing toward the bilayer center, although starting from the various geometries (Figure 4). The averaged distances between

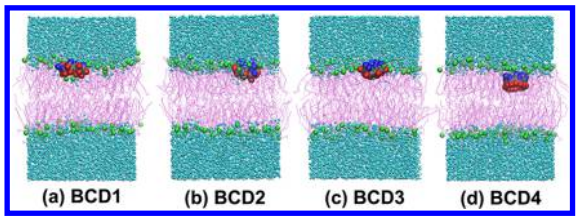

Figure 4. Last snapshots of (a) BCD1-(d) BCD4 simulations were extracted at 1 μs. The primary rim of βCD, secondary rim of βCD, phosphorus atoms of lipid, and water molecules are presented by blue, red, green, and cyan spheres, respectively. The purple lines represent the POPC lipid molecules.

COMs of the βCD molecule and the bilayer as well as the tilt angle of the βCD molecule with respect to the bilayer are presented in Table 1. In agreement with our results, in the simulations of cholesterol extraction from the lipid monolayer or the bilayer, the head-to-head βCD dimer adsorbed on the membrane surface, however; the dimer oriented its primary rim toward the bilayer surface instead.[49] Based on spectroscopic study and *ab initio* calculations, Mascetti et al. suggested that the βCD molecules preferred to stack in parallel to the pure cholesterol, mixed 1,2-dimyristoyl-*sn*-glycero-3-phosphoglycerol (DMPG)/cholesterol, and mixed 1,2-dimyristoyl-*sn*-glycero-3-phosphocholin (DMPC)/cholesterol lipid monolayers.[15]

Next, the behavior of the βCD molecule and the effect of βCD insertion inside the bilayer were studied. Therefore, βCD was placed at the bilayer's center with the $\vec{r}$ vector alignments in parallel (BCD4) and perpendicular (BCD5) to the bilayer normal. For the BCD4 system, the βCD molecule is able to form hydrogen bonds with the glycerol-ester groups of the lipid bilayer and moved toward the water−lipid interface within 10 ns (in Figure 3(d)). The equilibrium location of βCD was 1.0 nm from the bilayer center corresponding to the position of the glycerol-ester group. No bilayer deformation has been observed within a simulation time of one microsecond. Unlike the BCD5 system (Figure 5), the βCD molecule was initially oriented in perpendicular to the bilayer normal; therefore, hydroxyl groups of the βCD formed hydrogen bonds with the lipid heads of both bilayer leaflets. At a longer simulation time, the βCD molecule rotated to be in parallel to the bilayer normal, and a water pore across the lipid bilayer could be formed (Figure 5(b)).

II. The Interaction of the βCD Molecule with the Lipid bilayer. *Hydrogen Bonding Interactions.* The number of hydrogen bonds (H-bonds) between βCD, its rims, and the components of lipid head groups (phosphate and glycerol-ester moieties) were calculated using the usual geometric restrictions

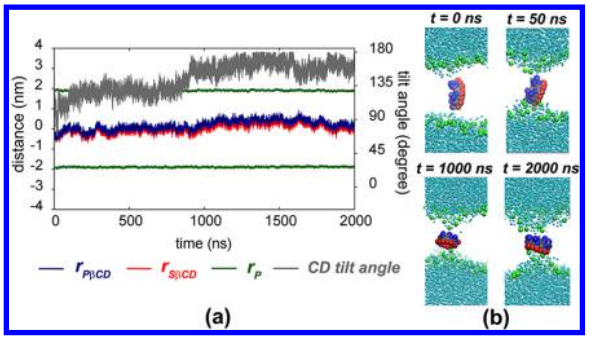

Figure 5. (a) Dynamics behavior of βCD starting from the perpendicular orientation in the lipid bilayer (BCD5). (b) Water pore formation induced by βCD at a longer simulation time, where the cyan sphere represents the water molecules, while the blue, red, and green spheres are symbolized as the atoms on primary and secondary rims of βCD and phosphorus of lipid head groups, respectively.

for hydrogen bonding. A hydrogen bond is defined by the distance between the donor and the acceptor (r_{HB}) < 0.35 nm and the deviation from the linearity <30°. The distance value of 0.35 nm corresponds to the first minimum of the radial distribution function (RDF) of water. Figure 6 shows the

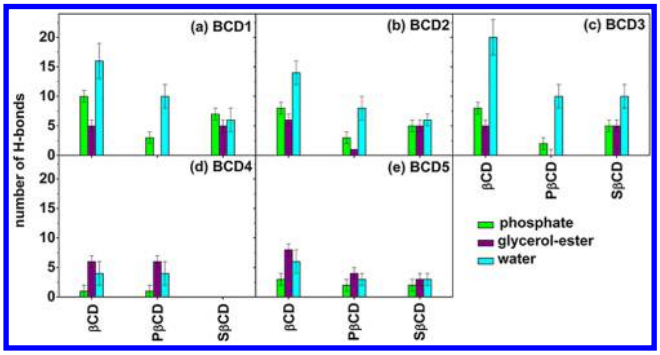

Figure 6. Hydrogen bond contribution of the interactions between the βCD molecule and phosphate (green) and glycerol-ester groups (purple) of the lipid and the solvating water molecules (cyan) for the systems (a) BCD1-(e) BCD5.

averaged number of hydrogen bonds at the last 500 ns and 1 μs for the systems of BCD1-BCD4 and BCD5, respectively. The βCD molecules in the BCD1-BCD3 systems interacted with the lipid headgroup with the hydroxyl groups at the secondary rim, and it was more preferred to form hydrogen bonds with phosphate groups than with glycerol-ester groups. On the other hand, this finding may suggest that the βCD interacted with the lipid surface stronger than the βCD dimer in the cholesterol extraction.[49] In the BCD4 and BCD5 systems, the primary rim of βCD is associated with the glycerol-ester group of the lipid bilayer. This is in good agreement with the results of the

Table 1. Average Values of the Focused Parameters on βCD-Lipid Interactions for All Simulations (BCD1-BCD5) over the MD Production Period

systems/properties	$r_{\beta CD}$ (nm)	$r_{P\beta CD}$ (nm)	$r_{S\beta CD}$ (nm)	tilt angle (degree)
BCD1 (500−1000 ns)	1.50 ± 0.10	1.54 ± 0.10	1.40 ± 0.10	163.6 ± 8.0
BCD2 (500−1000 ns)	1.55 ± 0.13	1.61 ± 0.13	1.49 ± 0.13	148.8 ± 7.6
BCD3 (500−1000 ns)	1.65 ± 0.12	1.72 ± 0.12	1.54 ± 0.12	167.4 ± 5.9
BCD4 (500−1000 ns)	1.08 ± 0.13	1.17 ± 0.13	0.96 ± 0.13	157.0 ± 11.1
BCD5 (1000−2000 ns)	0.30 ± 0.14	0.37 ± 0.15	0.20 ± 0.12	161.4 ± 7.4

DOI: 10.1021/acs.jcim.5b00152
J. Chem. Inf. Model. 2015, 55, 1894−1902

simulation snapshots and the permeate depths of the βCD molecule into the bilayer. Interestingly, the number of hydrogen bonds of βCD with water molecules significantly decreased from 16 to 5 when the βCD molecule translocated from water−lipid interface into the bilayer. In conclusion, the results of the hydrogen bonds suggest the translocation of βCD deeply into the hydrophobic region of the lipid bilayer is unfavorable.

The Influence of the βCD on the Lipid Membrane Properties. To study the influence of βCD on the bilayer structure, the two dimension (2D) density on the *xz*-plane of the βCD molecule, some POPC components (i.e., phosphate groups and glycerol-ester groups), and water were plotted in Figure 7 as well as the plots on the *xy*-plane in Figure S2

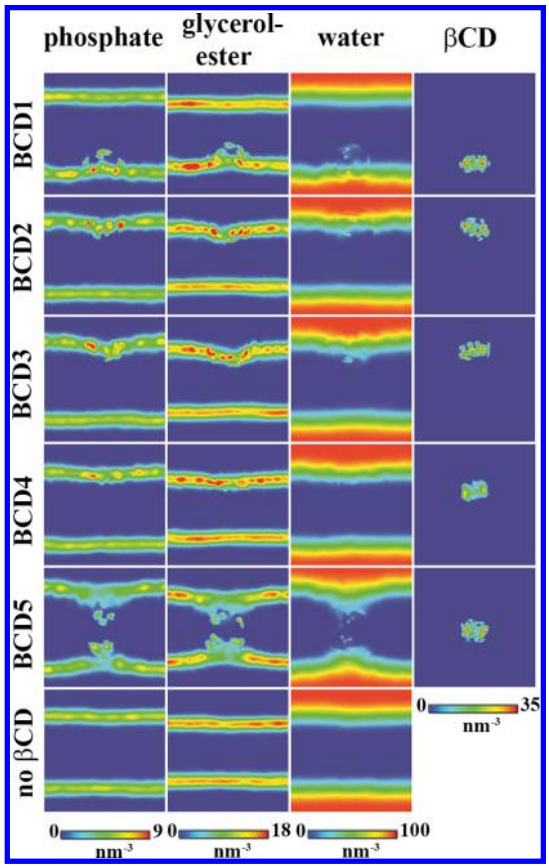

Figure 7. 2D-density maps on the *xz*-plane of the phosphate groups, glycerol-ester groups, water, and the βCD molecule for the BCD1-BCD5 systems, while those of the simulation of the POPC bilayer without βCD were given for comparison.

Supporting Information. The local thickness of the POPC bilayer on the *xy*-plane was also analyzed by means of the Voronoi algorithm[73] as shown in Figure 8. All analyses were computed from the last 100 ns of trajectories after removing the motion of the βCD molecule. The adsorption of one βCD molecule on the lipid bilayer cannot deform the membrane structure as seen by the insignificant change of 2D-density maps and the bilayer thickness of the BCD1-BCD3 ($r_{\beta CD}$ ∼ 1.50−1.65 nm) relative to the simulation of the POPC bilayer without βCD. The association of βCD on the lipid surface slightly induced the decrease of membrane thickness at the βCD location. When the βCD stayed underneath the glycerol-ester groups in the BCD4 system (the distance from the bilayer center, $r_{\beta CD}$ of ∼1.08 nm) it caused less disturbance on the lipid bilayer. In contradictory, the tilted βCD in the BCD5 system could bind with the lipid head groups causing the dramatic change in lipid thickness and inducing a water pore formation. In addition, the 2D-denstity maps (Figure 7 and Figure S2) could confirm that the βCD molecule in the BCD1-BCD3 systems preferred to stay at the bilayer surface with the hydroxyl rim tilted toward the bilayer center. The density maps on the *xy*-plane (Figure S2) showed that a few head groups of POPC molecules occupied inside the βCD cavity and 7−9 POPC molecules bound outside the βCD cavity. The ability of the cyclodextrin to uptake lipid or cholesterol from the biomembrane had been intensively demonstrated by *in vitro*, *in vivo*, and *in silico* studies.[47,74−76] This extraction may induce the pore formation or membrane change which had been reported by the leakage of potassium and hemoglobin at high concentration of cyclodextrins.[47]

Moreover, to investigate the dynamical property of the βCD influence on the POPC bilayer, we calculated the diffusion coefficient of the βCD molecule. The mean squared displacement (MSD) for 100 ns at the last of the BCD1-BCD5 systems and also the simulation of βCD in water were plotted and then fitted based on Einstein's relation $\langle r^2 \rangle \sim 4Dt$, where D is the diffusion coefficient, and t is time. The calculation is presented in the average of the diffusion coefficient by fitting of MSD every 20 ns. The results showed that the βCD diffusion coefficient in the water of our simulation is $(0.280 \pm 0.170) \times 10^{-9}$ m^2/s. This value is in the same magnitude as the experimental data.[77] The diffusion coefficient of βCD in the lipid phase, $(0.019 \pm 0.006) \times 10^{-9}$ m^2/s, is 1 order of magnitude smaller than in water. The slow diffusion of βCD in the lipid phase is related to strong binding of βCD with the lipid molecules.

III. The Conformational Change of the βCD Molecule. To investigate the conformational change of the βCD molecule, we determined the intramolecular hydrogen bonds obtained by the number of hydrogen bonds of the secondary rim between the adjacent glucoses. The intramolecular hydrogen bonds are related to the stability of the CD molecule.[78,79] The number of intramolecular hydrogen bonds of the BCD1-BCD3 systems was decreased continuously until there were no bonds left when the βCD molecule was attaching to the bilayer surface. The loss of this interaction was due to the preferable hydrogen bond formation between βCD and lipid head groups as well as water molecules[59,80−82] (Figure 6) and resulted in the structural deformation as shown in Figure 9. The root-mean-square displacement (RMSD) of the hydroxyl side chains on each rim and glycosidic oxygens (O1) with respect to its anhydrous structure (in Table 2) showed that the primary rim of βCD was more flexible than the other one.[80] The solvating water molecules affected the flexibility of the βCD structure for both side chain rims and the O1 core. In addition, the area of the βCD cavity was calculated by the following equation

$$A = \frac{\pi}{7} \sum_{i=1}^{7} r_i^2 \tag{1}$$

where r_i is the distance between each hydroxyl group and the center of the O1 atoms, and the hydroxyl groups at 6- and 3-positions are used for representing the cavity area of primary and secondary rims, respectively. The cavity areas of the βCD molecule in water, water−lipid interface, and lipid phase are summarized in Table 2. As expected for the truncated cone

DOI: 10.1021/acs.jcim.5b00152
J. Chem. Inf. Model. 2015, 55, 1894−1902

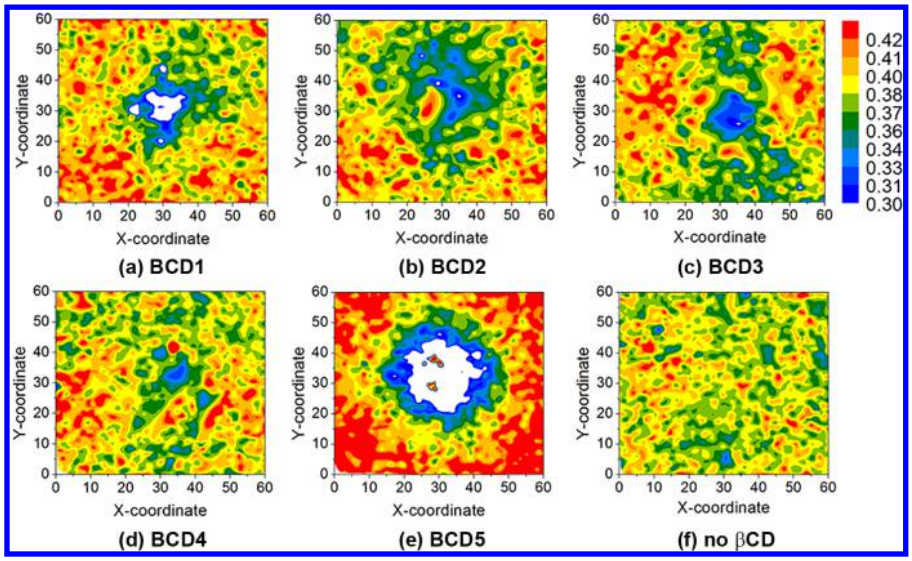

Figure 8. Local lipid thickness of the POPC bilayer in the systems with and without βCD ((a) BCD1-(e) BCD5 and (f) no βCD) where the βCD was located around the box center.

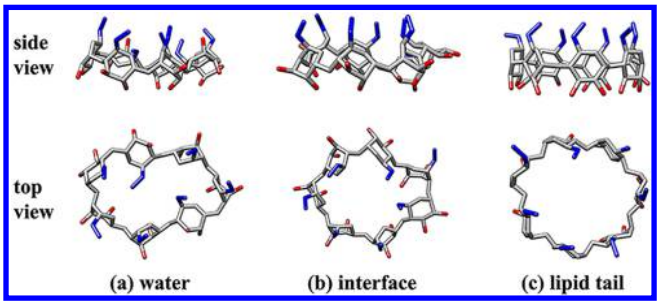

Figure 9. BCD in water was independently simulated for 500 ns, and the last MD snapshot was shown in (a). The last snapshots of βCD molecules obtained from the simulations of BCD3 and BCD4 for representing the βCD structure in lipid−water interface and lipid tail region as (b) and (c), respectively. The primary and secondary rims of the βCD molecule were labeled in blue and red, respectively. The backbone atoms of βCD molecules were represented in gray.

geometry of the βCD molecule, the cavity area of the secondary rim was larger than that of the primary rim about 1.5-fold in water and lipid phases, whereas the shape of the βCD molecule in the lipid tail resembled a cylinder. The area cavities of the secondary rim in the lipid phase were ∼15% and ∼25% smaller than in water and water−lipid interface, respectively. These findings may be related to the mechanism of drug release in which the open and closed states of the secondary rim of the βCD molecule at different phases may play an important role.

CONCLUSION

Based on the MD simulations of the βCD molecule with the lipid bilayer in the microsecond time scale, we found that the βCD molecule spontaneously permeated toward the lipid surface but did not further proceed into the bilayer tail region in agreement with free energy calculations.[49] No structural distortion of the bilayer could be observed when the βCD molecule attached to the bilayer surface. In contrast, the water pore formation in the lipid bilayer possibly occurred when the βCD molecule stayed inside the bilayer. The simulation results also showed that the secondary rim of the βCD molecule mainly contributed to the βCD-lipid interactions in which 5−7 hydrogen bonds between the secondary rim and the lipid heads were always found for the whole length of simulation time. Interestingly, the conformations of the βCD molecule changed at various solvation phases (water, water-bilayer interface, and bilayer) because of the loss of the intramolecular hydrogen bonds. An enlargement of area cavity at the water-bilayer interface could be observed. These findings might be related to the mechanism of drug releasing; however, there is still more work to be done in order to understand the function of βCD as a potential drug carrier.

ASSOCIATED CONTENT

Supporting Information

The Supporting Information is available free of charge on the ACS Publications website at DOI: 10.1021/acs.jcim.5b00152.

Figures S1 and S2, Table S1, and references (PDF)

AUTHOR INFORMATION

Corresponding Authors

*Phone: (J.W.) 66-2562-5555 ext 3545. Fax: 66-2942-8029. E-mail: jirasak.w@ku.ac.th.

*Phone: (T.R.) 66-2218-5426. Fax: 66-2218-5418. E-mail: thanyada.r@Chula.ac.th, t.rungrotmongkol@gmail.com.

Table 2. RMSD and Cavity Area of the βCD Molecule on Each Hydroxyl Rim

		RMSD (nm)			cavity area (nm^2)		
systems	$r_{\beta CD}$	O1	1st	2nd	O1	1st	2nd
in water		0.12 ± 0.02	0.33 ± 0.04	0.25 ± 0.02	0.93 ± 0.04	1.19 ± 0.12	1.56 ± 0.11
at interface	1.59 ± 0.10	0.10 ± 0.01	0.29 ± 0.01	0.23 ± 0.01	0.86 ± 0.03	1.36 ± 0.06	1.69 ± 0.03
in lipid tail	1.00 ± 0.10	0.06 ± 0.01	0.17 ± 0.02	0.08 ± 0.02	0.80 ± 0.02	1.35 ± 0.07	1.35 ± 0.04

DOI: 10.1021/acs.jcim.5b00152
J. Chem. Inf. Model. 2015, 55, 1894−1902

Notes

The authors declare no competing financial interest.

■ ACKNOWLEDGMENTS

This work was financially supported by the 90th anniversary of the Chulalongkorn University fund, the Ratchadaphiseksomphot Endowment Fund, and Asia Research Center (ARC) at Chulalongkorn University and Kasetsart University Research and Development Institute (KURDI) at Kasetsart University. J.W. gratefully acknowledges financial support from the Faculty of Science and Kasetsart University for the grant no. RFG1-8. T.R. thanks the Thailand Research Fund (IRG5780008 and MRG5580223). We also acknowledge the Computational Chemistry Unit Cell (CCUC) at Chulalongkorn University, the Computational Biophysics Group at Kasetsart University, and the Vienna Scientific Cluster (VSC-2) Austria for computing facilities and resources.

■ REFERENCES

(1) Loftsson, T.; Brewster, M. E. Pharmaceutical Applications of Cyclodextrins: Basic Science and Product Development. *J. Pharm. Pharmacol.* **2010**, *62*, 1607−1621.

(2) Kurkov, S. V.; Loftsson, T. Cyclodextrins. *Int. J. Pharm. (Amsterdam, Neth.)* **2013**, *453*, 167−180.

(3) Davis, M. E.; Brewster, M. E. Cyclodextrin-based Pharmaceutics: Past, Present and Future. *Nat. Rev. Drug Discovery* **2004**, *3*, 1023−1035.

(4) Amidon, G. L.; Lennernas, H.; Shah, V. P.; Crison, J. R. A Theoretical Basis for a Biopharmaceutic Drug Classification: The Correlation of in Vitro Drug Product Dissolution and in Vivo Bioavailability. *Pharm. Res.* **1995**, *12*, 413−420.

(5) Tommasini, S.; Raneri, D.; Ficarra, R.; Calabro, M. L.; Stancanelli, R.; Ficarra, P. Improvement in Solubility and Dissolution Rate of Flavonoids by Complexation with beta-Cyclodextrin. *J. Pharm. Biomed. Anal.* **2004**, *35*, 379−387.

(6) Zhang, Q.-F.; Nie, H.-C.; Shangguang, X.-C.; Yin, Z.-P.; Zheng, G.-D.; Chen, J.-G. Aqueous Solubility and Stability Enhancement of Astilbin through Complexation with Cyclodextrins. *J. Agric. Food Chem.* **2013**, *61*, 151−156.

(7) Patro, N. M.; Sultana, A.; Terao, K.; Nakata, D.; Jo, A.; Urano, A.; Ishida, Y.; Gorantla, R. N.; Pandit, V.; Devi, K.; Rohit, S.; Grewal, B. K.; Sophia, E. M.; Suresh, A.; Ekbote, V. K.; Suresh, S. Comparison and Correlation of in Vitro, in Vivo and in Silico Evaluations of Alpha, Beta and Gamma Cyclodextrin Complexes of Curcumin. *J. Inclusion Phenom. Macrocyclic Chem.* **2014**, *78*, 471−483.

(8) Danciu, C.; Soica, C.; Oltean, M.; Avram, S.; Borcan, F.; Csanyi, E.; Ambrus, R.; Zupko, I.; Muntean, D.; Dehelean, C. A.; Craina, M.; Popovici, R. A. Genistein in 1:1 Inclusion Complexes with Ramified Cyclodextrins: Theoretical, Physicochemical and Biological Evaluation. *Int. J. Mol. Sci.* **2014**, *15*, 1962−1982.

(9) de Souza Siqueira Quintans, J.; Menezes, P. P.; Santos, M. R. V.; Bonjardim, L. R.; Almeida, J. R. G. S.; Gelain, D. P.; Araújo, A.A.d.S.; Quintans-Júnior, L. J. Improvement of p-Cymene Antinociceptive and Anti-inflammatory Effects by Inclusion in β-Cyclodextrin. *Phytomedicine* **2013**, *20*, 436−440.

(10) Dreassi, E.; Zizzari, A. T.; Mori, M.; Filippi, I.; Belfiore, A.; Naldini, A.; Carraro, F.; Santucci, A.; Schenone, S.; Botta, M. 2-Hydroxypropyl-β-cyclodextrin Strongly Improves Water Solubility and Anti-proliferative Activity of Pyrazolo[3,4-d]pyrimidines Src-Abl Dual Inhibitors. *Eur. J. Med. Chem.* **2010**, *45*, 5958−5964.

(11) Loftsson, T.; Brewster, M. E. Pharmaceutical Applications of Cyclodextrins: Effects on Drug Permeation through Biological Membranes. *J. Pharm. Pharmacol.* **2011**, *63*, 1119−1135.

(12) Loftsson, T. Drug Permeation through Biomembranes: Cyclodextrins and the Unstirred Water Layer. *Pharmazie* **2012**, *67*, 363−370.

(13) Lipinski, C. A.; Lombardo, F.; Dominy, B. W.; Feeney, P. J. Experimental and Computational Approaches to Estimate Solubility and Permeability in Drug Discovery and Development Settings. *Adv. Drug Delivery Rev.* **1997**, *23*, 3−25.

(14) Yancey, P. G.; Rodrigueza, W. V.; Kilsdonk, E. P.; Stoudt, G. W.; Johnson, W. J.; Phillips, M. C.; Rothblat, G. H. Cellular Cholesterol Efflux Mediated by Cyclodextrins. Demonstration of Kinetic Pools and Mechanism of Efflux. *J. Biol. Chem.* **1996**, *271*, 16026−16034.

(15) Mascetti, J.; Castano, S.; Cavagnat, D.; Desbat, B. Organization of β-Cyclodextrin under Pure Cholesterol, DMPC, or DMPG and Mixed Cholesterol/Phospholipid Monolayers. *Langmuir* **2008**, *24*, 9616−9622.

(16) Wong-ekkabut, J.; Xu, Z.; Triampo, W.; Tang, I. M.; Tieleman, D. P.; Monticelli, L. Effect of Lipid Peroxidation on the Properties of Lipid Bilayers: A Molecular Dynamics Study. *Biophys. J.* **2007**, *93*, 4225−4236.

(17) Karplus, M.; McCammon, J. A. Molecular Dynamics Simulations of Biomolecules. *Nat. Struct. Biol.* **2002**, *9*, 646−652.

(18) Woods, R. J. Computational Carbohydrate Chemistry: What Theoretical Methods Can Tell Us. *Glycoconjugate J.* **1998**, *15*, 209−216.

(19) Tieleman, D. P.; Berendsen, H. J. A Molecular Dynamics Study of the Pores Formed by Escherichia coli OmpF Porin in a Fully Hydrated Palmitoyloleoylphosphatidylcholine Bilayer. *Biophys. J.* **1998**, *74*, 2786−2801.

(20) Khajeh, A.; Modarress, H. Effect of Cholesterol on Behavior of 5-Fluorouracil (5-FU) in a DMPC Lipid Bilayer, A Molecular Dynamics Study. *Biophys. Chem.* **2014**, *187*−*188*, 43−50.

(21) Orsi, M.; Sanderson, W. E.; Essex, J. W. Permeability of Small Molecules through a Lipid Bilayer: A Multiscale Simulation Study. *J. Phys. Chem. B* **2009**, *113*, 12019−12029.

(22) Nisoh, N.; Karttunen, M.; Monticelli, L.; Wong-ekkabut, J. Lipid Monolayer Disruption Caused by Aggregated Carbon Nanoparticles. *RSC Adv.* **2015**, *5*, 11676−11685.

(23) Wong-ekkabut, J.; Baoukina, S.; Triampo, W.; Tang, I. M.; Tieleman, D. P.; Monticelli, L. Computer Simulation Study of Fullerene Translocation through Lipid Membranes. *Nat. Nanotechnol.* **2008**, *3*, 363−368.

(24) Jarerattanachat, V.; Karttunen, M.; Wong-ekkabut, J. Molecular Dynamics Study of Oxidized Lipid Bilayers in NaCl Solution. *J. Phys. Chem. B* **2013**, *117*, 8490−8501.

(25) Wei, C.; Pohorille, A. Permeation of Membranes by Ribose and its Diastereomers. *J. Am. Chem. Soc.* **2009**, *131*, 10237−10245.

(26) Ivanov, P.; Atanassov, E.; Jaime, C. Computational Study on the Conformations of CD38 and Inclusion Complexes of some Lower-size Large-ring Cyclodextrins. *J. Mol. Struct.* **2014**, *1056-1057*, 238−245.

(27) Gotsev, M. G.; Ivanov, P. M. Molecular Dynamics of Large-ring Cyclodextrins: Principal Component Analysis of the Conformational Interconversions. *J. Phys. Chem. B* **2009**, *113*, 5752−5759.

(28) Ivanov, P. M.; Jaime, C. Insights into the Structure of Large-ring Cyclodextrins through Molecular Dynamics Simulations in Solution. *J. Phys. Chem. B* **2004**, *108*, 6261−6274.

(29) Nutho, B.; Khuntawee, W.; Rungnim, C.; Pongsawasdi, P.; Wolschann, P.; Karpfen, A.; Kungwan, N.; Rungrotmongkol, T. Binding Mode and Free Energy Prediction of Fisetin/β-cyclodextrin Inclusion Complexes. *Beilstein J. Org. Chem.* **2014**, *10*, 2789−2799.

(30) Sangpheak, W.; Khuntawee, W.; Wolschann, P.; Pongsawasdi, P.; Rungrotmongkol, T. Enhanced Stability of a Naringenin/2,6-dimethyl beta-Cyclodextrin Inclusion Complex: Molecular Dynamics and Free Energy Calculations based on MM- and QM-PBSA/GBSA. *J. Mol. Graphics Modell.* **2014**, *50*, 10−15.

(31) Chen, W.; Chang, C.-E.; Gilson, M. K. Calculation of Cyclodextrin Binding Affinities: Energy, Entropy, and Implications for Drug Design. *Biophys. J.* **2004**, *87*, 3035−3049.

(32) Zhang, H.; Tan, T.; Hetényi, C.; van der Spoel, D. Quantification of Solvent Contribution to the Stability of Noncovalent Complexes. *J. Chem. Theory Comput.* **2013**, *9*, 4542−4551.

(33) Zhang, H.; Tan, T.; Feng, W.; van der Spoel, D. Molecular Recognition in Different Environments: β-Cyclodextrin Dimer

DOI: 10.1021/acs.jcim.5b00152
J. Chem. Inf. Model. 2015, 55, 1894−1902

Formation in Organic Solvents. *J. Phys. Chem. B* **2012**, *116*, 12684−12693.
(34) Zhang, H.; Feng, W.; Li, C.; Tan, T. Investigation of the Inclusions of Puerarin and Daidzin with β-Cyclodextrin by Molecular Dynamics Simulation. *J. Phys. Chem. B* **2010**, *114*, 4876−4883.
(35) dos Santos, C.; Buera, M. P.; Mazzobre, M. F. Phase Solubility Studies and Stability of Cholesterol/β-Cyclodextrin Inclusion Complexes. *J. Sci. Food Agric.* **2011**, *91*, 2551−2557.
(36) Banerjee, R.; Chakraborty, H.; Sarkar, M. Host−Guest Complexation of Oxicam NSAIDs with β-Cyclodextrin. *Biopolymers* **2004**, *75*, 355−365.
(37) Karoyo, A. H.; Borisov, A. S.; Wilson, L. D.; Hazendonk, P. Formation of Host-Guest Complexes of β-Cyclodextrin and Perfluorooctanoic Acid. *J. Phys. Chem. B* **2011**, *115*, 9511−9527.
(38) Barbiric, D. J.; Castro, E. A.; de Rossi, R. H. A Molecular Mechanics Study of 1:1 Complexes between Azobenzene Derivatives and beta-Cyclodextrin. *J. Mol. Struct.: THEOCHEM* **2000**, *532*, 171−181.
(39) Kubo, Y.; Sugasaki, A.; Ikeda, M.; Sugiyasu, K.; Sonoda, K.; Ikeda, A.; Takeuchi, M.; Shinkai, S. Cooperative C-60 Binding to a Porphyrin Tetramer Arranged around a p-terphenyl Axis in 1:2 Host-Guest Stoichiometry. *Org. Lett.* **2002**, *4*, 925−928.
(40) Suzuki, M.; Ohmori, H.; Kajtar, M.; Szejtli, J.; Vikmon, M. The Association of Inclusion Complexes of Cyclodextrins with Azo Dyes. *J. Inclusion Phenom. Mol. Recognit. Chem.* **1994**, *18*, 255−264.
(41) Giastas, P.; Mourtzis, N.; Yannakopoulou, K.; Mavridis, I. Pseudorotaxanes of β-Cyclodextrin with Diamino End-functionalized Oligo-phenyl and -benzyl Compounds in Solution and in the Solid State. *J. Inclusion Phenom. Mol. Recognit. Chem.* **2002**, *44*, 247−250.
(42) Onnainty, R.; Schenfeld, E. M.; Quevedo, M. A.; Fernández, M. A.; Longhi, M. R.; Granero, G. E. Characterization of the Hydrochlorothiazide: β-Cyclodextrin Inclusion Complex. Experimental and Theoretical Methods. *J. Phys. Chem. B* **2013**, *117*, 206−217.
(43) Zidovetzki, R.; Levitan, I. Use of Cyclodextrins to Manipulate Plasma Membrane Cholesterol Content: Evidence, Misconceptions and Control Strategies. *Biochim. Biophys. Acta, Biomembr.* **2007**, *1768*, 1311−1324.
(44) Atger, V. M.; de la Llera Moya, M.; Stoudt, G. W.; Rodrigueza, W. V.; Phillips, M. C.; Rothblat, G. H. Cyclodextrins as Catalysts for the Removal of Cholesterol from Macrophage Foam Cells. *J. Clin. Invest.* **1997**, *99*, 773−780.
(45) Leventis, R.; Silvius, J. R. Use of Cyclodextrins to Monitor Transbilayer Movement and Differential Lipid Affinities of Cholesterol. *Biophys. J.* **2001**, *81*, 2257−2267.
(46) Ohvo, H.; Slotte, J. P. Cyclodextrin-Mediated Removal of Sterols from Monolayers: Effects of Sterol Structure and Phospholipids on Desorption Rate. *Biochemistry* **1996**, *35*, 8018−8024.
(47) Ohtani, Y.; Irie, T.; Uekama, K.; Fukunaga, K.; Pitha, J. Differential Effects of α-, β- and γ-Cyclodextrins on Human Erythrocytes. *Eur. J. Biochem.* **1989**, *186*, 17−22.
(48) López, C. A.; de Vries, A. H.; Marrink, S. J. Molecular Mechanism of Cyclodextrin Mediated Cholesterol Extraction. *PLoS Comput. Biol.* **2011**, *7*, e1002020.
(49) López, C. A.; de Vries, A. H.; Marrink, S. J. Computational Microscopy of Cyclodextrin Mediated Cholesterol Extraction from Lipid Model Membranes. *Sci. Rep.* **2013**, *3*, 2071.
(50) Pourmousa, M.; Wong-ekkabut, J.; Patra, M.; Karttunen, M. Molecular Dynamic Studies of Transportan Interacting with a DPPC Lipid Bilayer. *J. Phys. Chem. B* **2013**, *117*, 230−241.
(51) Karami, L.; Jalili, S. Effects of Cholesterol Concentration on the Interaction of Cytarabine with Lipid Membranes: A Molecular Dynamics Simulation Study. *J. Biomol. Struct. Dyn.* **2015**, *33*, 1254−1268.
(52) Bennett, W. F. D.; Tieleman, D. P. Water Defect and Pore Formation in Atomistic and Coarse-grained Lipid Membranes: Pushing the Limits of Coarse Graining. *J. Chem. Theory Comput.* **2011**, *7*, 2981−2988.
(53) Snor, W.; Liedl, E.; Weiss-Greiler, P.; Karpfen, A.; Viernstein, H.; Wolschann, P. On the Structure of Anhydrous β-Cyclodextrin. *Chem. Phys. Lett.* **2007**, *441*, 159−162.
(54) Hess, B.; Kutzner, C.; van der Spoel, D.; Lindahl, E. GROMACS 4: Algorithms for Highly Efficient, Load-balanced, and Scalable Molecular Simulation. *J. Chem. Theory Comput.* **2008**, *4*, 435−447.
(55) Berger, O.; Edholm, O.; Jähnig, F. Molecular Dynamics Simulations of a Fluid Bilayer of Dipalmitoylphosphatidylcholine at Full Hydration, Constant Pressure, and Constant Temperature. *Biophys. J.* **1997**, *72*, 2002−2013.
(56) Oostenbrink, C.; Villa, A.; Mark, A. E.; van Gunsteren, W. F. A Biomolecular Force Field Based on the Free Enthalpy of Hydration and Solvation: the GROMOS Force-field Parameter Sets 53A5 and 53A6. *J. Comput. Chem.* **2004**, *25*, 1656−1676.
(57) Lins, R. D.; Hunenberger, P. H. A New GROMOS Force Field for Hexopyranose-based Carbohydrates. *J. Comput. Chem.* **2005**, *26*, 1400−1412.
(58) Betzel, C.; Saenger, W.; Hingerty, B. E.; Brown, G. M. Topography of Cyclodextrin Inclusion Complexes, Part 20. Circular and Flip-flop Hydrogen Bonding in.beta.-Cyclodextrin Undecahydrate: a Neutron Diffraction Study. *J. Am. Chem. Soc.* **1984**, *106*, 7545−7557.
(59) Yong, C. W.; Washington, C.; Smith, W. Structural Behaviour of 2-Hydroxypropyl-β-Cyclodextrin in Water: Molecular Dynamics Simulation Studies. *Pharm. Res.* **2008**, *25*, 1092−1099.
(60) Cezard, C.; Trivelli, X.; Aubry, F.; Djedaini-Pilard, F.; Dupradeau, F.-Y. Molecular Dynamics Studies of Native and Substituted Cyclodextrins in Different Media: 1. Charge Derivation and Force Field Performances. *Phys. Chem. Chem. Phys.* **2011**, *13*, 15103−15121.
(61) Mixcoha, E.; Campos-Teran, J.; Pineiro, A. Surface Adsorption and Bulk Aggregation of Cyclodextrins by Computational Molecular Dynamics Simulations as a Function of Temperature: alpha-CD vs beta-CD. *J. Phys. Chem. B* **2014**, *118*, 6999−7011.
(62) Berendsen, H. J. C.; Postma, J. P. M.; van Gunsteren, W. F.; Hermans, J. Interaction Models for Water in Relation to Protein Hydration. In *Intermolecular Forces*; Pullman, B., Ed.; Springer: Netherlands, 1981; Vol. *14*, Chapter 21, pp 331−342.
(63) Bussi, G.; Donadio, D.; Parrinello, M. Canonical Sampling through Velocity Rescaling. *J. Chem. Phys.* **2007**, *126*, 014101.
(64) Bussi, G.; Zykova-Timan, T.; Parrinello, M. Isothermal-isobaric Molecular Dynamics using Stochastic Velocity Rescaling. *J. Chem. Phys.* **2009**, *130*, 074101.
(65) Berendsen, H. J. C.; Postma, J. P. M.; van Gunsteren, W. F.; DiNola, A.; Haak, J. R. Molecular Dynamics with Coupling to an External Bath. *J. Chem. Phys.* **1984**, *81*, 3684−3690.
(66) Darden, T.; York, D.; Pedersen, L. Particle mesh Ewald: An N·log (N) Method for Ewald Sums in Large Systems. *J. Chem. Phys.* **1993**, *98*, 10089−10092.
(67) Essmann, U.; Perera, L.; Berkowitz, M. L.; Darden, T.; Lee, H.; Pedersen, L. G. A Smooth Particle Mesh Ewald Method. *J. Chem. Phys.* **1995**, *103*, 8577−8593.
(68) Karttunen, M.; Rottler, J.; Vattulainen, I.; Sagui, C. Electrostatics in Biomolecular Simulations: Where Are We Now and Where Are We Heading? *Curr. Top. Membr.* **2008**, *60*, 49−89.
(69) Hess, B.; Bekker, H.; Berendsen, H. J. C.; Fraaije, J. G. E. M. LINCS: A Linear Constraint Solver for Molecular Simulations. *J. Comput. Chem.* **1997**, *18*, 1463−1472.
(70) Cino, E. A.; Choy, W. Y.; Karttunen, M. Comparison of Secondary Structure Formation using 10 Different Force Fields in Microsecond Molecular Dynamics Simulations. *J. Chem. Theory Comput.* **2012**, *8*, 2725−2740.
(71) Wong-ekkabut, J.; Karttunen, M. Assessment of Common Simulation Protocols for Simulations of Nanopores, Membrane Proteins, and Channels. *J. Chem. Theory Comput.* **2012**, *8*, 2905−2911.
(72) Humphrey, W.; Dalke, A.; Schulten, K. VMD: Visual Molecular Dynamics. *J. Mol. Graphics* **1996**, *14*, 33−38.
(73) Lukat, G.; Krüger, J.; Sommer, B. APL@Voro: A Voronoi-based Membrane Analysis Tool for GROMACS Trajectories. *J. Chem. Inf. Model.* **2013**, *53*, 2908−2925.

DOI: 10.1021/acs.jcim.5b00152
J. Chem. Inf. Model. 2015, 55, 1894−1902

(74) Frank, D. W.; Gray, J. E.; Weaver, R. N. Cyclodextrin Nephrosis in Rat. *Am. J. Pathol.* **1976**, *83*, 367−382.
(75) Legendre, J. Y.; Rault, I.; Petit, A.; Luijten, W.; Demuynck, I.; Horvath, S.; Ginot, Y. M.; Cuine, A. Effects of β-Cyclodextrins on Skin: Implications for the Transdermal Delivery of Piribedil and a Novel Cognition Enhancing-drug, S-9977. *Eur. J. Pharm. Sci.* **1995**, *3*, 311−322.
(76) Irie, T.; Uekama, K. Pharmaceutical Applications of Cyclodextrins. III. Toxicological Issues and Safety Evaluation. *J. Pharm. Sci.* **1997**, *86*, 147−62.
(77) Ribeiro, A. C. F.; Leaist, D. G.; Esteso, M. A.; Lobo, V. M. M.; Valente, A. J. M.; Santos, C. I. A. V.; Cabral, A.M.T.D.P.V.; Veiga, F. J. B. Binary Mutual Diffusion Coefficients of Aqueous Solutions of β-Cyclodextrin at Temperatures from 298.15 to 312.15 K. *J. Chem. Eng. Data* **2006**, *51*, 1368−1371.
(78) Chacko, K. K.; Saenger, W. Topography of Cyclodextrin Inclusion Complexes. 15. Crystal and Molecular Structure of the Cyclohexaamylose-7.57 Water Complex, Form III. Four- and Six-membered Circular Hydrogen Bonds. *J. Am. Chem. Soc.* **1981**, *103*, 1708−1715.
(79) Dodziuk, H. Molecules with Holes − Cyclodextrins. In *Cyclodextrins and Their Complexes*; Wiley-VCH Verlag GmbH & Co. KGaA: 2006; pp 1−30.
(80) Koehler, J. E.; Saenger, W.; van Gunsteren, W. F. Molecular Dynamics Simulation of Crystalline beta-Cyclodextrin Dodecahydrate at 293 and 120 K. *Eur. Biophys. J.* **1987**, *15*, 211−224.
(81) Koehler, J. E. H.; Saenger, W.; van Gunsteren, W. F. The Flip-flop Hydrogen Bonding Phenomenon. *Eur. Biophys. J.* **1988**, *16*, 153−168.
(82) Saenger, W.; Jacob, J.; Gessler, K.; Steiner, T.; Hoffmann, D.; Sanbe, H.; Koizumi, K.; Smith, S. M.; Takaha, T. Structures of the Common Cyclodextrins and Their Larger Analogues-Beyond the Doughnut. *Chem. Rev. (Washington, DC, U. S.)* **1998**, *98*, 1787−1802.

DOI: 10.1021/acs.jcim.5b00152
J. Chem. Inf. Model. 2015, 55, 1894−1902